Optimizing the Parameters of CIGS Solar Cells Using One-Dimension AFORS-HET Program

Rafea A. Munef[1*], Maad M. Ameen[2], Rosure Borhanalden Abdulrahman[3*], Haneen Waleed[4], Abdulhadi M. Ghelab[5]

Abstract

In this study, the performance of the AZO/ZnO/CdS/CIGS solar cell configuration was measured by using the AFORS-HET numerical simulation program, which aimed to formulate an optimal design. The numerical simulation of the aforementioned solar cell arrangement demonstrates that it is possible to achieve an efficiency of 9.28% with a thickness of 1µm, this result is consistent with the experimental conclusion (where the efficiency was 9.65% for a thickness of 1µm). Through the use of simulation results, we improved the above-mentioned cell by changing the thickness, concentration, and band gap. It shows that the maximum efficiency (Eff) of this solar cell can reach 17.46% during the optimization for this configuration, which can be obtained at a thickness of 3µm for CIGS layer and at 1.5 AM standard illumination.

Key Words: CIGS-Simulation Solar Cell, AFORS-HET, Quaternary Chalcogenides, Maximum Efficiency.

DOI Number: 10.14704/nq.2022.20.2.NQ22027 **NeuroQuantology 2022; 20(2):69-75**

Introduction

The physical mechanism complexity of the that govern the solar cell devices gave to an argent for using solar simulation programs which is a necessity fundamental in designing and analyszing the solar cells (Soga, 2006). The paper aims to provide a theoretical framework based on a relevance between materials properties and the solar cell operations, in addition, to determine the physical parameters that influence its performance. Numerical CIGS thin-film solar cells by a one-dimensional AFORS-HET (automat for simulation of heterostructures) program offers some sufficient insights into understanding how changing the parameters will affect the overall solar cell's outputs If they are uniformly illuminated. Interest in CIGS thin-film solar cells began in 1981 when Mickels and Chen obatined 9.4% performance by an evaporation technology (Mickelsen & Chen, 1981). P-type CIGS semiconductor shows a blue shift of absorption edge with high optical absorption coefficient along with optimum energy gap appropriate for the solar cell (Kato, 2017). In addition to its advantages and uses in various applications, photovoltaic cells can be made very flexible and lightweight by using metal foil or polymer substrates, which is desirable to construct integrated structures, moreover exhibited high radiation resistance compared to crystalline silicon-based solar cells (Powalla et al., 2017). The additional advantage of CIGS-based solar cells is that require much lower materials in relation to the standard Si-based solar cells in addition to fewer energy production requirements (Powalla et al., 2017).

Among all thin film chalcogenide solar cells, Cd-free CIGS solar cells produce a superior power conversion efficiency of about 23.35% (Green et al., 2021).

Corresponding author: Rafea A. Munef[1*] & Rosure Borhanalden Abdulrahman[3*]
Address: [1*,2,3*,4,5]Department of Physics, College of Science, University of Kirkuk, Kirkuk, Iraq.
E-mail: [1*]rafeamonef@uokirkuk.edu.iq; [3*]rbabdulrahman@uokirkuk.edu.iq
Relevant conflicts of interest/financial disclosures: The authors declare that the research was conducted in the absence of any commercial or financial relationships that could be construed as a potential conflict of interest.
Received: 09 December 2021 **Accepted:** 12 January 2022

There are two major approaches to fabrrcate CIGS thin film deposition such as selenization and co-evaporation techniques (Kato, 2017; Niki et al., 2010). In the Selenization, the indium, metals copper, and gallium are initially deposited on a metalized glass substrate follwed by Selenization process. In the co-evaporation process, the CIGS layer forms directly through the thermal evaporation of all elements in a vacuum on a metalized glass substrate (Kato, 2017). The double-graded band gap (Ga gradient at the back side and S-rich layer at the front side of CIGS absorber layer) resists electron–hole recombination at the rear and front interfaces as well as assisting in carrier transportation and collection, which is beneficial to enhance solar cells efficiency (Khatri et al., 2015; Nagoya et al., 2001).

The thickness of 2nd generation thin film solar cells can be modified (from several nanometers up to ten micrometers) to have an insignificant thickness compared to traditional 1st generation Si-based solar cells (about 200 μm thick wafers). Studies showed that the thicknesses of the absorber and hole transport layer in addition to the doping level imapct on the solar cell performance (Bag et al., 2020; Zahoo & Saleh, 2021). This is the reason the thin film solar cells have less mass, amenablein addition, possess a limited prevemtion (Efaz1 et al., 2021).

AFORS-HET is a simulation program that has the ability to treat homojunction as well as heterojunctions semiconductors. The simulation program can handle interface recombination in addition to bulk recombination throughout introducing interface defects within the semiconductor layers. A thermionic emission or drift-diffusion interface model can be selected to illustrate a hole and electron transport through the semiconductor layers. The properties of the semiconductor layers are possibly an exponential, linear, Gaussian, or Error function. The program can calculate the front and back solar cell contact of the as a Schottky, insulator, or metal/insulator/ semiconductor boundary, which gave the simulation the flexibility to propose different experimental configurations. Since the program permits for use of various parameters thus the simulated measurements can match the real measurements (Stangl et al., 2010; Stangl & Leendertz, 2012).

The main objective in this work is to investigate the parameters which involve for improving CIGS solar cells using 1D- AFORS-HET simulation. We initiated the work with the examination the impact of the absorber layer thickness on CIGS PV cell performance. The merit of the simulation is to predict and test the device and the parameters which influence the results without device fabrication. To ensure reliable results of the simulation we took into consideration a comparison of Jiang Liu and his co-workers' experimental result (Liu et al., 2013) by using simulation, later we improved the output of the solar cell by changing some parameters.

Solar Cell Simulation

The semiconductor materials do not have constant characteristics always, whereas thin film solar cells include flaws that are precarious, as soon as increasing in the processing temperature in the production line the defects move within the device layers. Moreover, the interface between semiconductor layers in some solar cells significantly influences their characteristics (Stangl & Leendertz, 2012).

Solar cell simulation divides into: optical and electrical simulations, and each of them can be performed individually such as FDTD (Abdulrahman et al., 2013) and DEVICE simulation (Arjmand & McGuire, 2013). In the first step, a generation rate (numbers of electrons and holes made in a second and in a unit volume at a specific time and position) can be calculated by optical simulation within the semiconductor layers due to the absorption of light. According to the optical model which is selected for the simulation, impacts like internal or external reflections, internal surfaces light scattering, or coherent superposition of the propagating light can be taken into the consideration. In the second step, the generation rate in which obtained from the first step can be considered as an input for the electrical stimulation. By using electrical simulation, the carrier densities and the electric potential can be calculated for various boundary conditions in the semiconductor layers. The remaining solar cell internal quantities, including recombination rates, band diagrams, currents and phase shifts might be consequently estimated from the carrier densities and the electric potential (Stangl & Leendertz, 2012).

The solution for carrier densities and electric potential is found by solving the Poisson and the steadiness equations for electrons and holes. In 1964 and for the first time the numerical modeling for a semiconductor device was proposed by Gummel (Gummel, 1964). According to the selection of the recombination model for the simulation,

effects such as radiative recombination, Auger recombination (non-radiative recombination), or Shockley-Read-Hall (SRH recombination) recombination can be taken into account (Stangl & Leendertz, 2012).

Generation

When the heterostructure semiconductor layers are illuminated with an inputs of photon flux ($\emptyset(\lambda)$) the optical super-bandgap generation rate $G_n = G_p$ (when $hc/\lambda \geq E_g$) can be achieved by several methods: first, by Lambert-Beer absorption but with assigning an absorption coefficient α for each layer. Second, by taking into consideration the multiple reflections (coherent/incoherent reflections) within the layers, and designating the dielectric properties (n,k) for each layer. finally, this rate (when $hc/\lambda < E_g$) from a flaw to the valence and/or conduction band can be calculated using SRH recombination and it can be described by assigning optical emission coefficients $e_n^0(E), e_p^0(E) \neq 0$ for the defect state (Stangl & Leendertz, 2012):

$$\boldsymbol{e_n^0(E,x) = \sigma_n^0 N_C \emptyset(\lambda,x)\vartheta(E_C - E - hc/\lambda)} \quad (1)$$

$$\boldsymbol{e_p^0(E,x) = \sigma_p^0 N_V \emptyset(\lambda,x)\vartheta(E - E_V - hc/\lambda)} \quad (2)$$

$\sigma_{n,p}^0$: capture cross sections for electrons and holes capturing, $\emptyset(\lambda,x)$ incoming photon Flux of wavelength λ at the position x, $N_{V,C}$: valence/conduction band density, $E_{V,C}$: valence/conduction band energy, ϑ: $\vartheta(E) = 1$ for $E \leq 0, \vartheta(E) = 0$ for $E > 0$.

Recombination

Radiative recombination (band recombined to band), Auger recombination (band to band recombination) and SHR recombination (defect states within the semiconductor band gap) may take place directly from the transmission of band into the valence band (Stangl & Leendertz, 2012):

$$\boldsymbol{R_{n,p}(x,t) = R_{n,p}^{direct}(x,t) + R_{n,p}^{SHR}(x,t)} \quad (3)$$

Band to band rate r^{BB} and the Auger rate constants r_n^A, r_p^A should be specified for a direct recombination (Stangl & Leendertz, 2012):

$$\boldsymbol{R_{n,p}^{direct}(x,t) = R_{n,p}^{direct}(x) + \tilde{R}_{n,p}^{direct}(x)e^{i\omega t}} \quad (4)$$

To calculate SHR recombination an arbitrary number of defect states should be distributed within the semiconductor band gap moreover, its requires to specify energetic defect distribution $N_t(E)$ within the semiconductor band gap of each defect and the capture coefficients $c_{n,p} = v_{n,p}\sigma_{n,p}$ ($v_{n,p}$: thermal velocity $\sigma_{n,p}$: capture cross section) for its electron/hole. The SRH recombination rate because of the defects state can be calculated (Stangl & Leendertz, 2012):

$$\boldsymbol{R_{n,p}^{SRH}(x,t) = R_{n,p}^{SRH}(x) + \tilde{R}_{n,p}^{SRH}(x)e^{i\omega t}} \quad (5)$$

The distribution function $f_t(E,x,t)$ is obtained from the SHR theory which describes the occupied defect states (Stangl & Leendertz, 2012):

$$\boldsymbol{f_t(E,x,t) = f_t(E,x) + \tilde{f}_t(E,x)e^{i\omega t}} \quad (6)$$

Interfaces

The electron and hole current transportation within the semiconductor layer interface can be determined by drift-diffusion and interface models of the thermionic emission.

The Electron and Hole Current determined by Drift Diffusion Interface Model

An interface layer of a definite thickness was employed in this model, in which the properties of the material can vary linearly within the semiconductor layers. The semiconductor layers can be treated similar to bulk semiconducting layer (drift/diffusion driven), where the currents transport within the heterojunction interface since the distribution of interface defects are homogeneous within the layer. The currents of the electron and hole should be calculated which driven from the gradient of the counterpart quasi fermi energies E_{Fn}, because the band gap E_g, the electron affinity χ, and the transmission and/or valence band densities N_C, N_V within the interface layer relies upon the position x (Stangl & Leendertz, 2012):

$$\boldsymbol{E_{Fn}(x) = -q\,\chi(x) + q\varphi(x) - kTln\frac{n(x)}{N_c(x)}} \quad (7)$$

$$\boldsymbol{E_{Fp}(x) = -q\,\chi(x) + q\varphi(x) - E_g(x) + kTln\frac{p(x)}{N_V(x)}} \quad (8)$$

The Electron and Hole Current Driven by Thermionic Emission Interface Model

By thermionic emission model, the electron and hole current transportation across a heterojunction interface can be calculated over the interface energetic barrier, that is the conduction and valence band offset $\Delta E_{C,V}$ (Stangl & Leendertz, 2012):

$$\boldsymbol{\Delta E_C = q\chi^+ - q\chi^-} \quad (9)$$

$$\boldsymbol{\Delta E_V = E_g^+ - E_g^- + q\chi^+ - q\chi^-} \quad (10)$$

Solar Cell Configuration

In general, the cell consists of a thin buffer layer CdS deposited on a CIGS absorbent layer and a zinc oxide layer ZnO inserted between the CdS and ZnO: Al layer, and the front contact is made of Al to prevent current leakage and the back contact from Mo. Figure (1) shows the simulated solar cell structure configuration of this study. The key structure sections are the CIGS absorption layer. Table 1. gives all parameters used for the solar cell structure Using these parameters, the solar cell was simulated to get the best efficiency.

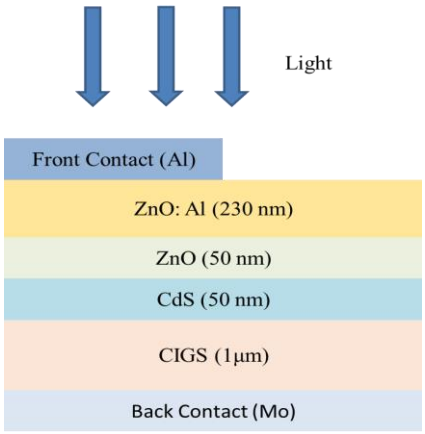

Fig. 1. The solar cell structure configuration

Table 1. Parameters of solar cell AZO/ZnO/CdS/CIGS (Bouchaour et al., 2019; Dabbabi et al., 2017; Devi et al., 2018; Fathi et al., 2015; Frisk et al., 2014; Mebelson & Elampari, 2019; Touafek & Mahamadi, 2014).

Parameters	Symbol (unit)	CIGS	AZO	ZnO	CdS
Thickness	d	1μm	230nm	50nm	50nm
Dielectric constant	dk	13.6	9	9	10
Electron affinity	chi(eV)	4.4	4.5	4.6	4.2
Band gap	Eg(eV)	1.3	3.3	3.3	2.42
Density of state in CB	$Nc(cm^{-3})$	2.2×10^{18}	3×10^{18}	2.2×10^{18}	1.3×10^{18}
Density of state in VB	$Nv(cm^{-3})$	1.5×10^{19}	1.7×10^{18}	1.8×10^{19}	9.1×10^{19}
Electron mobility	$\mu_n(cm^2/Vs)$	100	100	100	72
Hole mobility	$\mu_p(cm^2/Vs)$	25	25	25	20
Acceptor concentration	$N_a(cm^{-3})$	5×10^{15}	0	0	0
Donor concentration	$N_d(cm^{-3})$	0	1×10^{20}	1×10^{18}	1×10^{18}
Thermal velocity of electron and hole	$V_{th}(cm/s)$	1×10^{7}	1×10^{7}	1×10^{7}	1×10^{7}
Refractive index	n			AFORS- HET	
Extinction coefficient	k				

Results and Discussion

Comparing the Results of the AFORS-HET Program with the Results of the Practical Research

In this study, the practical research was compared (Jiang Liu) (Liu et al., 2013) with the one-dimensional AFORS-HET program, the thickness of the absorption layer CIGS was 1 μm and energy gap 1.3 eV. It was shown through the results that the simulation program matches research as in the table 2.

Table 2. Results of the Simulation with the results of the experimentally research

	V_{oc} [mV]	J_{sc} [mA/cm^2]	FF%	η%
Simulation	453.9	32.3	63.31	9.28
Experimentally	452.42	32.16	66.32	9.65

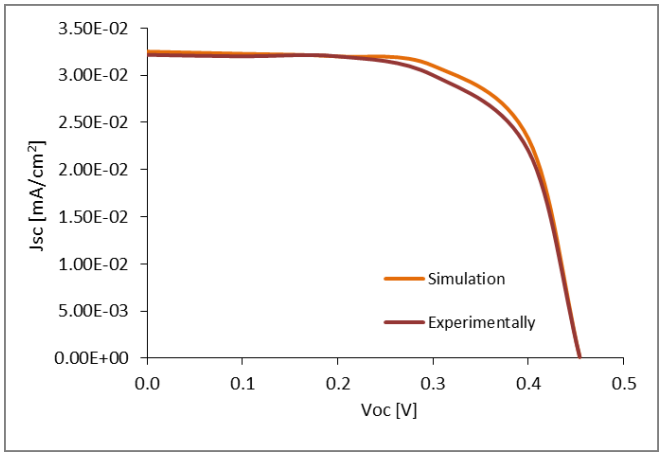

Fig. 2. Current and voltage (J-V) diagram prior to improving

Absorber Layer Thickness Impact on the Efficiency of Solar Cell

The simulation result reveals that if the absorber layer thickness changes from (500nm-3 μm) the open circuit voltage, filling factor and short circuit

current and competence increase. When the front face for the solar cell is illuminated with high-energy photons, they will penetrate the absorber layer, and later electron-hole recombination process occurs at the device back face.

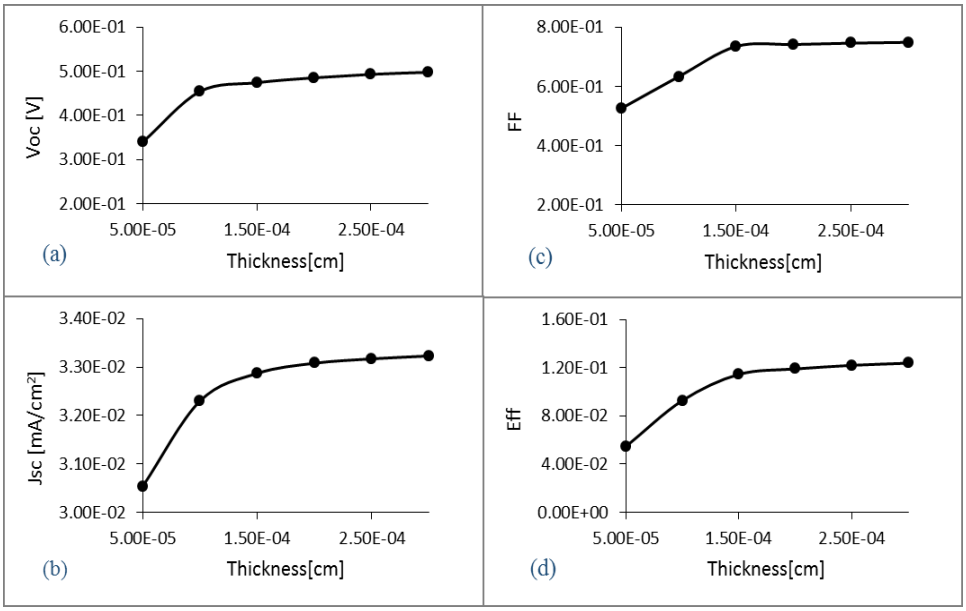

Fig. 2. Absorber layer CIGS influence on (a) V_{oc} , (b) J_{sc}, (c) FF, (d) Eff

Effect Hole Density of Absorber Layer on Solar Cell

Fig: 3- depicts the impact of absorber layer hole density on electrical parameters such as open circuit voltage, short circuit current, fill factor, and the competence. It is observed from the results that when the absorption layer thickness 3 μm, the electrical parameters V_{oc}, FF, Eff increase when the hole density increase from N_a= (5×10^{14}-5×10^{16})cm^{-3} and as a consequence of decreasing the diffusion length. The J_{sc} decreases because the recombination process grows with the growth of the hole density.

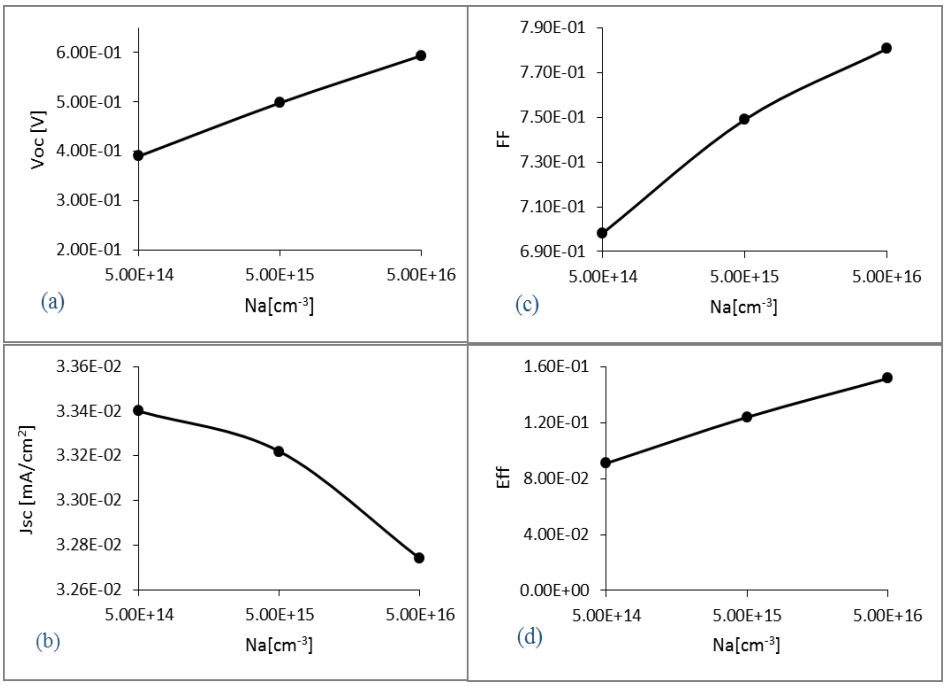

Fig. 3. Effect hole density on absorber layer CIGS on both (a) V_{oc}, (b) J_{sc}, (c) FF,(d) Eff

Absorber Layer CIGS Band Gap effect on Solar Cell

The pure CIGS 1.04 eV band gap reaching 1.65 eV when Ge in CIGS is doped. We fixed all the parameters of the other layers with the band gap changing from (1-1.15) eV. Figure 4 reveal the effect of the band gap energy on short circuit current, open circuit voltage, fill factor, and the competence response, we can observe an increase in V_{oc}, J_{sc}, FF, and Eff with the rise in the band gap.

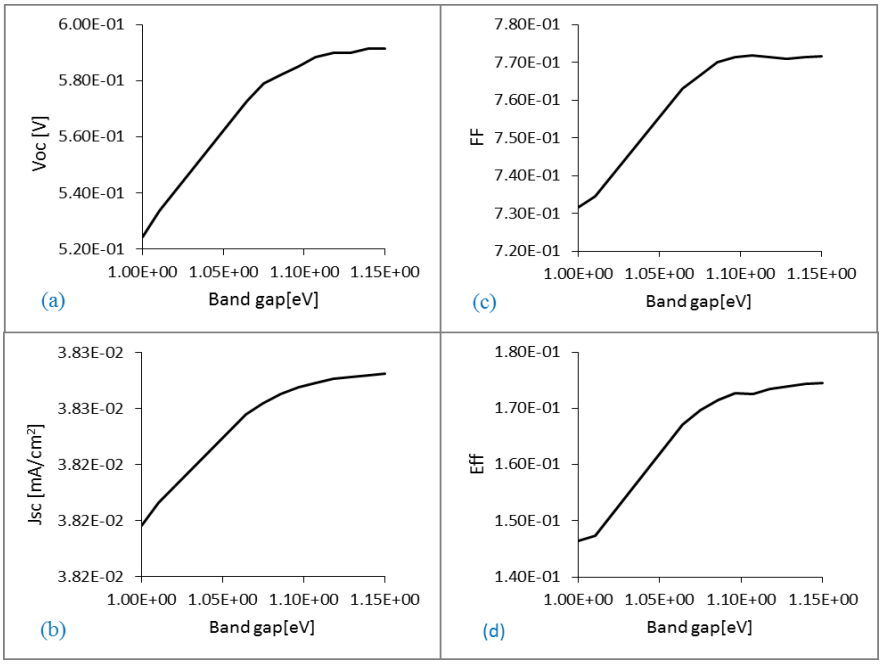

Fig. 4. CIGS band gap influence on (a) V_{oc} , (b) J_{sc}, (c) FF, (d) Eff

Conclusion

Using AFORS-HET program, the thickness influence, concentration, and energy gap on the competence of the solar cell were examined. After that, the best parameters of the absorption layer were determined. It was found that the change of thickness, concentration, and energy gap of the CIGS layer affects solar cell efficiency. We were capable of output of the CIGS cell structure improvement. Where the efficiency showed an improvement of Eff=17.46%, V_{oc}=591.4 mV, FF=77.15, J_{sc}=38.26 mA/cm^2.

References

Abdulrahman RB, Alagoz AS, Karabacak T. Enhanced light trapping in periodic aluminum nanorod arrays as cavity resonator. *Hague Journal on the Rule of Law* 2013; 1566(1): 0–5. https://doi.org/10.1557/opl.2013.878

Arjmand A, McGuire D. Complete optoelectronic simulation of patterned silicon solar cells. *13th International Conference on Numerical Simulation of Optoelectronic Devices. NUSOD 2013* 2013: 13–14. https://doi.org/10.1109/NUSOD.2013.6633100

Bag A, Radhakrishnan R, Nekovei R, Jeyakumar R. Effect of absorber layer, hole transport layer thicknesses, and its doping density on the performance of perovskite solar cells by device simulation. *Solar Energy* 2020; 196: 177–182. https://doi.org/10.1016/j.solener.2019.12.014

Bouchaour M, Merad L, Sari NEC. Influence of doping and thickness on the performance of CIGS PV cell. *International Journal of Energy and Environment* 2019; 13: 13–16.

Dabbabi S, Nasr, TB, Kamoun-Turki N. Parameters optimization of CIGS solar cell using 2D physical modeling. *Results in Physics* 2017; 7: 4020–4024. https://doi.org/10.1016/J.RINP.2017.06.057

Devi N, Aziz A, Datta S. Numerical modelling of CIGS/CdS solar cell. *AIP Conference Proceedings* 2018: 1953(1). https://doi.org/10.1063/1.5032967

Efaz ET, Rhaman MM, Al Imam S, Bashar KL, Kabir F, Mourtaza ME, Sakib SN, Mozahid FA. A review of primary technologies of thin-film solar cells. *Engineering Research Express* 2021: 3(3). https://doi.org/10.1088/2631-8695/AC2353

Fathi M, Abderrezek M, Djahli F, Ayad M. Study of Thin Film Solar Cells in High Temperature Condition. *Energy Procedia* 2015; 74: 1410–1417. https://doi.org/10.1016/J.EGYPRO.2015.07.788

Frisk C, Platzer-Björkman C, Olsson J, Szaniawski P, Wätjen JT, Fjällström V, Salomé P, Edoff M. Optimizing Ga-profiles for highly efficient Cu(In, Ga)Se_2 thin film solar cells in simple and complex defect models. *Journal of Physics D: Applied Physics* 2014: 47(48). https://doi.org/10.1088/0022-3727/47/48/485104

Green MA, Dunlop ED, Hohl-Ebinger J, Yoshita M, Kopidakis N, Hao X. Solar cell efficiency tables (Version 58). *Progress in Photovoltaics: Research and Applications* 2021; 29(7): 657-667. https://doi.org/10.1002/PIP.3444

Gummel HK. A Self-Consistent Iterative Scheme for One-Dimensional Steady State Transistor Calculations. *IEEE Transactions on Electron Devices* 1964; 11(10): 455–465. https://doi.org/10.1109/T-ED.1964.15364

Kato T. Cu(In,Ga)(Se,S)2 solar cell research in Solar Frontier: Progress and current status. *Japanese Journal of Applied Physics* 2017: 56. https://doi.org/10.7567/JJAP.56.04CA02

Khatri I, Matsuyama I, Yamaguchi H, Fukai H, Nakada T. Surface sulfurization on MBE-grown Cu(In1-x,Gax)Se2 thin films and devices. *Japanese Journal of Applied Physics* 2015: 54(8). https://doi.org/10.7567/JJAP.54.08KC10/XML

Liu J, Zhuang D, Luan H, Cao M, Xie M, Li X. Preparation of Cu(In,Ga)Se2 thin film by sputtering from Cu(In,Ga)Se2 quaternary target. *Progress in Natural Science: Materials International* 2013; 23(2): 133–138. https://doi.org/10.1016/J.PNSC.2013.02.006

Mebelson TJ, Elampari K. Numerical Simulation for Optimal Thickness Combination of CdS/ZnS Dual Buffer Layer CuInGaSe2 Solar Cell Using SCAPS 1D. *Indian Journal of Science and Technology* 2019; 12(45): 1–6. https://doi.org/10.17485/IJST/2019/V12I45/148395

Mickelsen RA, Chen WS. Development of a 9.4% efficient thin-film CuInSe2/CdS solar cell. *15th Photovoltaic Specialists Conference* 1981: 800–804.

Nagoya Y, Kushiya K, Tachiyuki M, Yamase O. Role of incorporated sulfur into the surface of Cu(InGa)Se_2 thin-film absorber. *Solar Energy Materials and Solar Cells* 2001; 67(1–4): 247–253. https://doi.org/10.1016/S0927-0248(00)00288-9

Niki S, Contreras M, Repins I, Powalla M, Kushiya K, Ishizuka S, Matsubara K. CIGS absorbers and processes. *Progress in Photovoltaics: Research and Applications* 2010; 18(6): 453–466. https://doi.org/10.1002/PIP.969

Powalla M, Paetel S, Hariskos D, Wuerz R, Kessler F, Lechner P, Wischmann W, Friedlmeier TM. Advances in Cost-Efficient Thin-Film Photovoltaics Based on Cu(In,Ga)Se_2. *Engineering* 2017; 3(4): 445–451. https://doi.org/10.1016/J.ENG.2017.04.015

Soga T. *Nanostructured materials for solar energy conversion*. Elsevier 2006.

Stangl R, Leendertz C. General Principles of Solar Cell Simulation and Introduction to AFORS-HET. *In Physics and Technology of Amorphous-Crystalline Heterostructure Silicon Solar Cells Springer, Berlin, Heidelberg* 2012: 445-458. https://doi.org/10.1007/978-3-642-22275-7_13

Stangl R, Leendertz C, Haschke J. Numerical Simulation of Solar Cells and Solar Cell Characterization Methods: the Open-Source on Demand Program AFORS-HET. *In Solar Energy* 2010: 310–352. https://doi.org/10.5772/8073

Touafek N, Mahamadi R. Back Surface Recombination Effect on the Ultra-Thin CIGS Solar Cells by SCAPS. *International Journal of Renewable Energy Research* 2014; 4: 958–964.

Zahoo RK, Saleh AN. Effect of Carrier Concentration and Thickness of Absorber Layer on Performance CBTS Solar Cell. *Turkish Journal of Computer and Mathematics Education* 2021; 12(10): 5056–5064.

Aziz SA, Ali RS, Abd AN. Characterization studies of nickel oxide nanostructure films prepared by electrolysis method for photo detectors applications. *NeuroQuantology* 2020; 18(2): 45-49.